Biosensors and Bioelectronics 151 (2020) 111971

Contents lists available at ScienceDirect

Biosensors and Bioelectronics

journal homepage: http://www.elsevier.com/locate/bios

D-amino acid electrochemical biosensor based on D-amino acid oxidase: Mechanism and high performance against enantiomer interference

Tingting Tian, Mingxia Liu, Lixia Chen, Fengjiao Zhang, Xin Yao, Hong Zhao, Xiangjun Li *

School of Chemical Sciences, University of Chinese Academy of Sciences, Beijing, 100049, China

ARTICLE INFO

Keywords:
Electrochemical biosensor
Chiral recognition
D-amino acid oxidase
Mechanism

ABSTRACT

For D-amino acid (DAA) electrochemical biosensors, it is necessary to achieve chiral recognition in racemic solutions or mixtures. However, common chiral recognition is only performed in a single isomer solution. Here, D-amino acid oxidase (DAAO) was used as a chiral selector, and carbon nanotubes (CNTs) as a signal amplifier to construct a non-mediator-style DAA biosensor. The biosensor showed high performance against enantiomer interference: in alanine (Ala) enantiomer mixtures, accurate quantification of D-Ala was achieved when the concentration ratio of L-Ala to D-Ala was 100. In Ala racemic solutions, the linear equation slope was almost consistent with that of standard D-Ala. This high performance was due to the combination of stereoselectivity (enzyme protein) and a catalytic reaction (redox center). The mechanism for the electrical signal change of the biosensor was explored and verified by cyclic voltammetry (CV). The results showed that (i) flavin adenine dinucleotide (FAD, redox center of DAAO) was a direct electroactive substance that produced a reduction peak current; in the presence of O_2, the amount of FAD increased leading to an increase of the reduction peak current. (ii) In the presence of DAA, the chemical reaction FAD + DAA → imino acids + $FADH_2$ occurred and consumed FAD, which resulted in its decrease; thus, the reduction peak current also decreased. Under the same oxygen concentration, the linear decrease of the reduction peak current in the presence of DAA was due to FAD consumption. The biosensor was used for practical analyses in milk and urine samples with satisfactory results.

1. Introduction

Chiral molecules are ubiquitous, in general, and are present in the basic components of life (amino acids, proteins, DNA), medicine, pesticides and new synthetic functional materials, but only one isomer exhibits activity or functionality; the other is ineffective and even cause side effects, so chiral analysis is of vital importance in life, drugs and materials sciences (Bergantini et al., 2018; Du et al., 2013; Hao et al., 2019; Zhang et al., 2017). Among the developed chiral analysis methods, electrochemical methods (electrochemical sensors) have been widely used in the field of chiral analysis because of their simple operation, fast response and easy miniaturization. The most critical element of the electrochemical sensor is the chiral selector which directly determines the performance of the sensor. There are many kinds of chiral selectors currently used for chiral recognition, including (i) natural polysaccharides, such as chitosan (CS) (Bao et al., 2016; Gholivand and Mohammadi-Behzad, 2015) and cyclodextrin (Tao et al., 2017; Wu and Kong, 2019; Zaidi, 2017), (ii) synthetic chiral polymers, such as 3, 4-methylenedioxymethamphetamine derivatives (Dong et al., 2017) and MOFs materials (Wu et al., 2017) and (iii) biological materials, such as chiral amino acids (Gou et al., 2016; Zhang et al., 2019), enzymes that catalyse chiral substrates (Arai et al., 1998; Zhu et al., 2017) and chiral specific nucleic acid aptamers (Challier et al., 2016; Tohala et al., 2015).

Most chiral selectors used for chiral recognition are based on interaction differences or stereo matching differences with enantiomers to achieve chiral recognition; the greater the difference, the better the recognition performance. However, these differences are so weak that it is difficult to convert them into electrical signal differences in the enantiomer mixture. Furthermore, another difficulty is that most electrochemical chiral sensors only perform in a single isomer (L- or D-isomer) solution, and chiral quantitative identification cannot be achieved in an enantiomer mixture (L- and D-isomer).

To solve this problem, researchers have focused on bio-enzymes that catalyse chiral substrates not only by weak interactions but also by stereospecific chemical reactions. These enzymes, such as DAAO (FAD-dependent oxidase)(Arai et al., 1998; Kiss and Ferenczy, 2019; Sacchi et al., 1998), which has a high degree of stereospecificity, can catalyse a variety of DAA molecules with different degrees of oxidation but are

* Corresponding author.
E-mail address: lixiangj@ucas.ac.cn (X. Li).

https://doi.org/10.1016/j.bios.2019.111971
Received 16 October 2019; Received in revised form 13 December 2019; Accepted 15 December 2019
Available online 17 December 2019

resistant to L-amino acid (LAA). The catalytic reaction formula is as follows (Moreno et al., 1996): $DAA + O_2 \xrightarrow{DAAO}$ imino acid + H_2O_2. Importantly, the redox center of DAAO can realize direct electron transfer (DET) on the surface of the electrode by producing an electrochemical signal. Furthermore, the electrochemical signal can be changed by a catalytic reaction of DAAO to DAA, and the electrochemical signal change has a linear relationship with the concentration of DAA in a certain range so that DAA can be determined quantitatively. Utilized in an electrochemical biosensor, DAAO has two advantages: (i) for non-electroactive DAA, the linear relationship between the electrical signal change of DAAO and DAA concentration can be utilized to realize its electrochemical detection, such as for D-Ala and (ii) for electroactive DAA, the electrical signal change of DAAO combined with the electrical signal of DAA itself can be utilized to realize dual electrochemical signal detection, such as for D-tryptophan.

At present, electrochemical biosensors based on DAAO have been studied for DAA chiral recognition (Pernot et al., 2008; Pundir et al., 2018; Zain et al., 2010), but quantitative identification in racemic solutions or mixtures have rarely been discussed. In addition, because of the diversity of redox mediators, studies mainly concentrated on the introduction of redox mediators, which mediate electron transfer of DAAO, H_2O_2 (a by-product of DAAO catalysis to DAA) or peroxidase to indirectly determine DAA (Fig. 1A) (Moreno-Guzmán et al., 2017; Nieh et al., 2013; Wcislo et al., 2007). However, a non-mediator-style DAA biosensor based on DAAO (Fig. 1B) has rarely been reported, despite its advantages of a simple electron transfer process and less electrode contamination.

Herein, a non-mediator-style DAA biosensor was constructed, which was simply modified layer of DAAO/CNTs composite film and a layer of Nafion (as a protective agent). The only electrical signal was produced by DET between the DAAO and electrode. As commonly used carbon materials in biosensors (Alim et al., 2018; Katz and Willner, 2004), CNTs with excellent conductivity, commercial availability and biocompatibility (Britto et al., 1999; Gupta et al., 2018; Nugent et al., 2001) was chosen as a signal amplifier. In our work, the electrical signal decreased with the increased DAA concentration. This phenomenon was consistent with the electrical signal change of a non-mediator-style glucose biosensor based on glucose oxidase (GOD, which is also an FAD-dependent oxidase), but was inconsistent with that of mediator-style DAA biosensors. For example, a non-mediator-style glucose biosensor based on GOD has a reduction peak current (at −0.517 V) that decreased with increasing glucose (Kang et al., 2009). However, with a mediator-style DAA biosensor based on DAAO and a mediator of pentacyanoferrate-bound poly (1-vinylimidazole) polymer (PVI[Fe(CN)$_5$]), the reduction peak current (at 0.1 V) increased with increasing DAA (Nieh et al., 2013). Because of this contradiction, the mechanism that caused the change in the reduction peak current was further explored by a CV analysis from the point when the reduction peak current was generated. In addition, the performance and practical applications for chiral DAA recognition were also studied.

2. Experimental

2.1. Reagents and materials

CS (Deacetylation degree ≥90%) was purchased from Sinopharm Chemical Reagent Co., Ltd (Shanghai, China). L-Ala, D-Ala, CNTs (>95% purity and ~50 μm long), Na_2HPO_4, NaH_2PO_4 and KCl were purchased from Aladdin Chemistry Co., Ltd (Shanghai, China). DAAO (from a porcine kidney, ≥1.5 units/mg solid) and Nafion solution (5 wt% in a mixture of low aliphatic alcohols and 45%water) were purchased from Sigma Aldrich Co (USA). The stock DAAO solution was prepared in phosphate buffer saline and stored at 4 °C. Acetic acid (>99.5%) was purchased from Beijing Chemical Reagent Co., Ltd (Beijing, China). All other chemicals were analytical grade and directly used without further purification. A milk sample was purchased from Jingdong Mall and a urine sample was donated from a healthy volunteer. Phosphate buffer saline with 0.1 M KCl (PBS 50 mM, pH 7.4) was used as a supporting electrolyte.

2.2. Fabrication of enzyme electrode

DAAO/CNTs solutions were prepared by mixing CNTs solutions (dispersing CNTs in a CS solution and ultrasonication for 20 min) with appropriate amounts of DAAO.

Electrode modification was conducted by casting appropriate amount of a DAAO/CNTs and Nafion solution onto the surface of a glass carbon electrode (GCE, 3 mm in diameter). The modified electrode was stored at 4 °C in PBS when not in use.

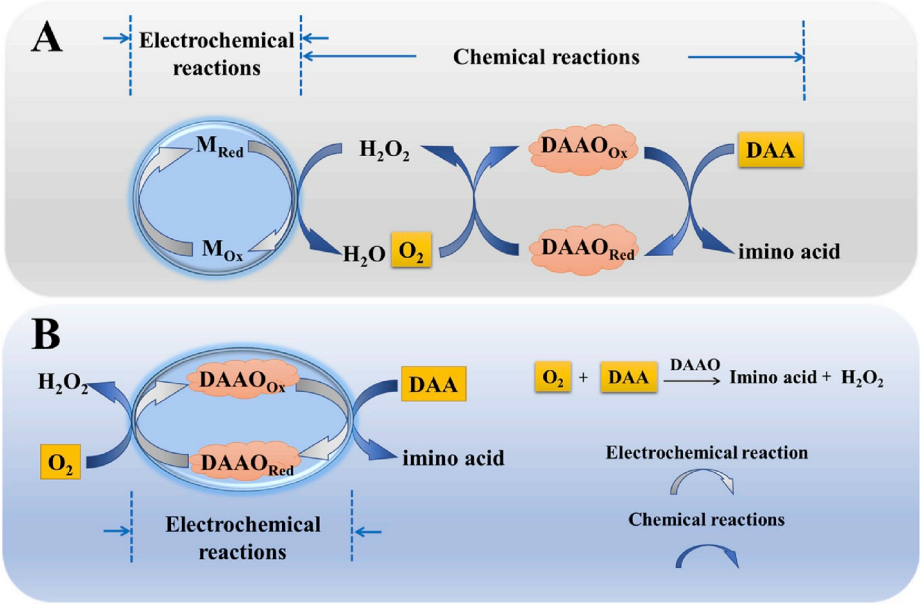

Fig. 1. (A) Indirect detection of DAA by mediator-style biosensors based on DAAO. (B) Direct detection of DAA by a non-mediator-style biosensor based on DAAO.

2.3. Electrochemical measurements

Electrochemical experiments were performed in a conventional three-electrode cell connected to a CHI-660E electrochemical workstation (CH Instruments, Inc., China) with the above GCEs as the working electrode, a saturated calomel electrode (SCE) as the reference electrode and a platinum wire as the counter electrode. N_2-saturated PBS and N_2-saturated DAA solutions were prepared by purging with high-purity nitrogen for at least 30 min, and air-saturated PBS and the air-saturated DAA solutions were without any pretreatment. CV measurements were performed in an air-saturated solution at 35 °C unless otherwise stated.

3. Results and discussion

3.1. Electrochemical signal of DAAO

A DET between DAAO and the surface of the electrode was hardly achieved. The redox center of DAAO is deeply embedded into the large three-dimensional structure of the enzyme molecule, which leads to a significant decrease in the electron transfer capacity (Liu et al., 2005). To improve this capacity, CNTs with excellent conductivity, commercial availability and biocompatibility were chosen as the signal amplifier.

There are two points to consider, (i) the DAAO electrochemical conversion mechanism and (ii) verification of the CNT effect. (i) For the electrochemical conversion of DAAO, electrons transfer occurs in its redox center, FAD/$FADH_2$, which is known to exchange two protons and two electrons via a redox reaction (Degani and Heller, 1988; Iannlello et al., 1982; Liu and Ju, 2003). Fig. S1 shows the CV curve of FAD/CNTs/GCE. A pair of redox peaks was observed at approximately −0.5 V. Regarding DAAO/CNTs/GCE, the reduction peak potential moved negatively because of protein masking (Fig. S2). In general, both the potential and peak shapes were similar between DAAO/CNTs/GCE and FAD/CNTs/GCE. In addition, the peak potential of DAAO/CNTs/GCE linearly changed with a pH increase over a certain range (Fig. S3). The linear slope was close to the theoretical value of −58.6 mV/pH (Liu et al., 2007), suggesting that two protons and two electrons participated in the DET of DAAO. The consistencies of the potential, peak shapes and transfer process between DAAO/CNTs/GCE and FAD/CNTs/GCE, suggested that the DAAO electrochemical conversion was achieved with FAD/$FADH_2$ (Degani and Heller, 1988).

(ii) For effects of the CNTs that were studied, Fig. 2A shows the CV curves of GCE, DAAO/GCE and DAAO/CNTs/GCE in PBS. No peak appeared for the bare GCE, and a weak reduction peak appeared for DAAO/GCE, suggesting a weak DET of DAAO on the surface of the GCE. The reason for these results is that FAD was deeply embedded in a protective protein matrix (Andreu et al., 2007), resulting in difficult electron transfer with the electrode. However, the reduction peak for DAAO/CNTs/GCE increased by 1.9 times compared to that of DAAO/GCE, and the oxidation peak appeared, suggesting that the DET of DAAO on the surface of the electrode was obviously promoted. This promotion contributed to a high local density of electronic states in the CNTs and a large surface area of CNTs-based electrodes (Sa et al., 2019; Zhang et al., 2004). Fig. 2B shows the relationship between the reduction peak current and different concentrations of DAA for DAAO/GCE and DAAO/CNTs/GCE. For DAAO/GCE, the electrical signal response in DAA from 0 to 0.4 mM varies little (<1 μA). For DAAO/CNTs/GCE, the signal response magnitude was obviously enhanced and linearly related to different DAAs in a certain range, suggesting that CNTs can be successfully used as signal amplifiers.

Interestingly, the phenomenon that the reduction peak current decreased with increasing DAA (Fig. 3), was opposite with previous reports that the reduction peak current increased in mediator-style biosensors based on DAAO (Dominguez et al., 2001; Nieh et al., 2013). However, it was consistent with previously reported non-mediator-style glucose biosensors based on glucose oxidase (GOD, which is also a FAD-dependent oxidase) (Kang et al., 2009). The previous published paper attributed oxygen consumption in the solution as the reason for the decrease in the reduction peak current. However, in our system, the oxygen concentration in DAA solution at different concentrations was basically the same level (air-saturated), indicating that a decrease in oxygen concentration was not the key reason for our experimental phenomenon. To clarify the reason, reactions occurring on the electrode surface should be analysed in detail.

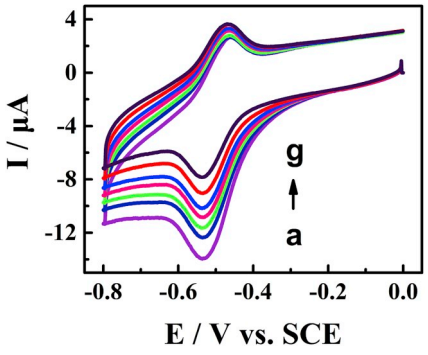

Fig. 3. CV curves of DAAO/CNTs/GCE in different concentrations of DAA (from a to g): 0, 0.08, 0.1, 0.2, 0.3, 0.4 and 0.5 mM.

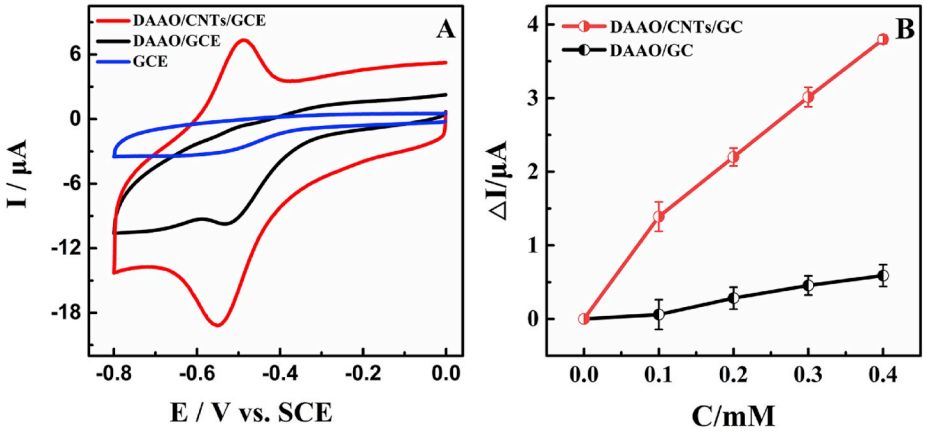

Fig. 2. (A) CV curves of bare GCE, DAAO/GCE and DAAO/CNTs/GCE in air-saturated PBS. (B) The electrical signal responses ($\triangle I = I_{PBS}-I_{DAA}$) of DAAO/GCE and DAAO/CNTs/GCE at different concentrations of DAA (from 0 to 0.4 mM).

3.2. Mechanism of the electrochemical signal change

As discussed above, DET of DAAO occurred in its redox center (FAD/$FADH_2$), where two protons and two electrons were exchanged. The transfer process can be described by two electrochemical reactions (Liu and Ju, 2003):

$$FAD + 2e^- + 2H^+ \rightarrow FADH_2 \quad (a)$$

$$FADH_2 \rightarrow FAD + 2e^- + 2H^+ \quad (b)$$

Since FAD obtained electrons from the electrode, electrochemical reaction (a) produced a reduction current. Correspondingly, electrochemical reaction (b) produced an oxidation current due to $FADH_2$ losing electrons on the electrode. In an air-saturated DAA solution, DAA and dissolved O_2 are involved in chemical reactions (Nieh et al., 2013):

$$FAD + DAA \rightarrow imino\ acid + FADH_2 \quad (c)$$

$$FADH_2 + O_2 \rightarrow FAD + H_2O_2 \quad (d)$$

By studying the effect of DAA and O_2 on FAD, the reason for the decrease in the reduction peak current will become clear. Therefore, CV experiments with four solutions (i) N_2-saturated PBS, (ii) N_2-saturated DAA solution, (iii) air-saturated PBS and (iv) air-saturated DAA solution were conducted to study the effects of O_2 and DAA.

The reaction processes and corresponding CV curves are shown in Fig. 4. (i) For N_2-saturated PBS, a pair of reversible redox peaks was observed in the CV curve due to electrochemical reactions (a) and (b) (Fig. 4A). (ii) For the N_2-saturated DAA solution, the reduction peak current decreased compared with that of (i) (Fig. 4B). This was because of the additional occurrence of chemical reaction (c). In chemical reaction (c), DAA competitively combined with FAD, which directly decreased the amount of FAD in electrochemical reaction (a) so that the reduction peak current decreased. Comparing (i) and (ii) showed that DAA decreased the reduction peak current of DAAO. (iii) For air-saturated PBS, the reduction peak current obviously increased

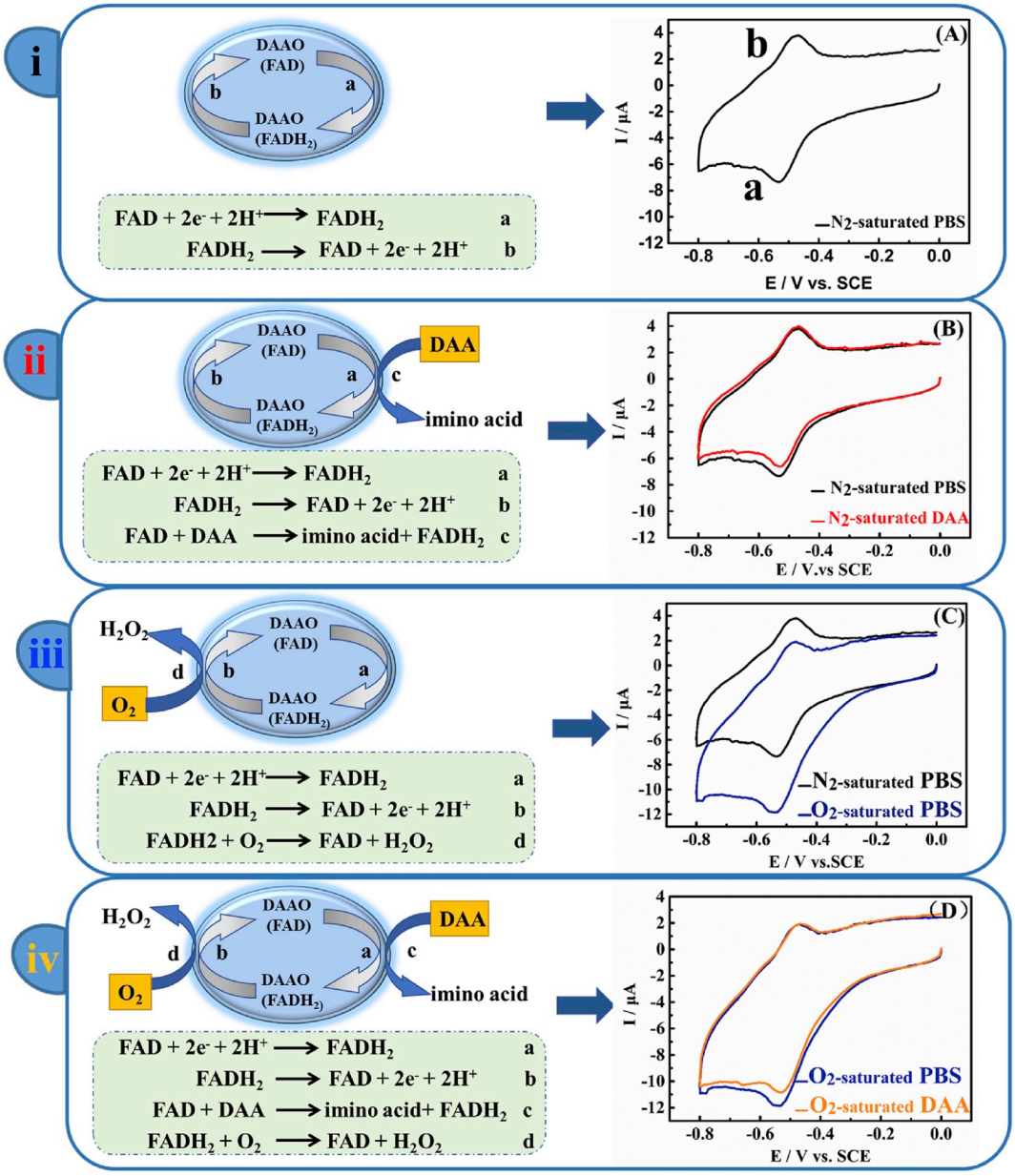

Fig. 4. Reaction process on the DAAO/CNTs/GCE surface in (i) N_2-saturated PBS, (ii) N_2-saturated DAA solution, (iii) air-saturated PBS and (iv) air-saturated DAA solution.

compared with that of (i) (Fig. 4C). This was because chemical reaction (d) occurred in addition to electrochemical reactions (a) and (b). In chemical reaction (d), O_2 combined with $FADH_2$ to produce FAD, which directly increased the amount of FAD in electrochemical reaction (a). A comparison of N_2-saturated and O_2-saturated PBS showed that O_2 increased the reduction peak current of DAAO. (iv) For air-saturated DAA solution, the reduction peak current decreased compared with that of (iii) (Fig. 4D) because of FAD competitive consumption by DAA in chemical reaction (c). A comparison of O_2-saturated PBS and O_2-saturated DAA solution showed that DAA decreased the reduction peak current of DAAO. In conclusion, two points should be noted: (i) O_2 increased the reduction peak current of the DAAO modified non-mediator style biosensor and (ii) regardless of the absence or presence of O_2, DAA addition will decrease the reduction peak current. Because the reduction peak current was generated by electron transfer between the electrode and FAD, FAD decreased due to the competitive combination with DAA, so the reduction peak current decreased. In our system, as DAA increased, more FAD was consumed so the reduction peak current decreased.

This mechanism is suitable for non-mediator-style biosensors based on (i) all kinds of FAD-dependent oxidases and (ii) the kind of enzyme that has a redox center that is electroactive, where its oxidation state is directly involved in the substrate catalytic reaction. Furthermore, this mechanism contributes to explaining the change of electrochemical signals in mediator-style electrochemical sensors.

3.3. Chiral recognition performance

Condition optimization was conducted for the electrode modification process, including the concentration of CNTs and the amount of DAAO deposition, and for the testing process, namely, variations in temperature, pH and the scan rate. We found that the amount of DAAO deposition and temperature were the two most influential factors, with an optimal DAAO deposition of 0.57 U and an optimal temperature of 35 °C utilized in this experiment, respectively. Thus, D-Ala sensors with excellent performance were finally obtained. The reduction peak current linearly decreased with the concentration of D-Ala from 9 μM to 600 μM (Fig. 5), and the detection limit was 7.91 μM (S/N = 3), which was of the same magnitude as that of mediator-style sensors (Wcislo et al., 2007).

To realize chiral recognition of D-Ala with high efficiency, it is necessary to discuss the interference of L-Ala. In our work, three experiments were conducted: (i) comparing the electrical signal responses caused by the same concentrations of L-Ala and D-Ala, (ii) mixing different concentrations of L-Ala with a fixed concentration of D-Ala, comparing the electrical signal response of this enantiomer mixtures with that of the D-Ala single isomer and (iii) studying the quantitative recognition of D-Ala in an Ala-racemic solution. As a result, in experiment (i), we found that the CV curves for different concentrations of L-Ala (0.1–0.5 mM) almost overlapped with that of PBS, while the CV curves for the corresponding D-Ala obviously changed (Fig. 6A); furthermore the electrical signal response in D-Ala was found to be significantly larger than that in L-Ala at the same concentration (Fig. 6B). In experiment (ii), different concentrations of L-Ala and 0.2 mM D-Ala were mixed, and the reduction peak currents in the enantiomer mixture were consistent with that of 0.2 mM D-Ala. When 20 mM of L-Ala was in the mixture, that is, the concentration ratio of L-Ala to D-Ala was 100, the reduction peak current was still almost identical to that of the 0.2 mM D-Ala single isomer (Fig. 6C). In experiment (iii), D-Ala determination was conducted in an Ala racemic solution. We found that the change in the electric signal response was linearly correlated with the concentration of D-Ala and that the slope was almost consistent with that of the standard D-Ala single solution (Fig. 6D). The results of these three experiments showed that: (i) the interference of L-Ala was negligible for quantitative detection of D-Ala in the enantiomer mixture and that (ii) the sensor could realize the quantitative recognition of D-Ala in a racemic solution.

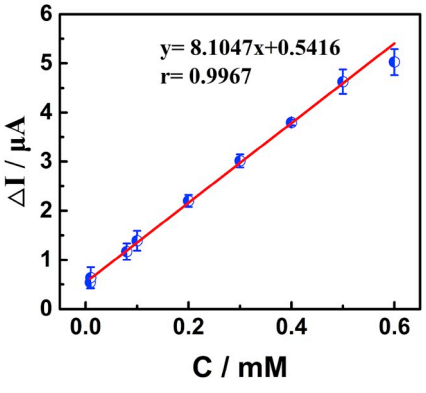

Fig. 5. Linear relationship between the electrical signal responses of DAAO/CNTs/GCE vs. the D-Ala concentration.

Actually, most electrochemical sensors are only performed in a single isomer solution because they cannot achieve quantitative chiral recognition in an enantiomer mixture or can only predict the percent content of a single isomer. Because the proposed sensor based on DAAO can effectively exclude interference due to LAA, we believe that other non-enzyme chiral selectors are based on a difference in interaction or stereo-specific matching towards enantiomers (Afkhami et al., 2015; Atta et al., 2019; Feng et al., 2014); by contrast, the advantage of a DAAO selector is the combination of stereo-selectivity and a chemical catalytic reaction. That is, the enzyme proteins achieve three-dimensional selectivity to the DAA and exclude LAA following the selected DAA oxidation by the internal catalytic center, which results in an electrical signal change of the redox center, so that the electrical signal change is directly related to the concentration of DAA. Therefore, the chiral recognition efficiency is greatly improved.

To evaluate the stability of the biosensor, the enzyme electrode was stored in a refrigerator at 4 °C, after 15 days and 20 days of storage, the electrical signal response remained at 96% and 94% of its original electrical signal, respectively. In addition, the reproducibility and repeatability of the electrical signal response were evaluated by intra-assay and inter-assay analyses at three concentration levels (0 mM, 0.1 mM and 0.5 mM). All of the RSD% were less than 7.5% (Table S1). These results showed satisfactory stability, reproducibility and repeatability of the proposed biosensor.

3.4. Sample analysis

In the process of D-Ala determination, although the proposed biosensor can effectively exclude the interference of L-Ala, DAAO can catalyse a variety of DAA molecules that cause uncontrollable interference and affect the accuracy of chiral recognition (Liu et al., 2017; Pollegioni et al., 2008). However, there is still an extensive need in practical application. First, the biosensor based on DAAO can be applied to measure the dynamic change of one kind of DAA. For example, D-serine (D-Ser) is an endogenous ligand for N-methyl-D-aspartate (NMDA) receptors (Bains and Oliet, 2007; Ishiwata et al., 2018; Mothet et al., 2000), and alterations in its concentration are related to several brain disorders. The level of D-Ser in cerebrospinal fluid of patients with a mental illness is significantly lower than that in normal people (Hashimoto et al., 2004). By detecting the electrical signal difference of cerebrospinal fluid in normal people and patients, the altered content of D-Ser can be determined so that disease information can be obtained to provide guidance for effective treatment (Quan et al., 2005). For another example, D-Ala is an important marker of food contamination, and the content of D-Ala is obviously increased while those of other DAAs are basically unchanged in contaminated food (Csapó et al., 1995; Gandolfi et al., 1994). By detecting the electrical signal difference in testing and normal food, the quality of the test food can be evaluated. Second, the

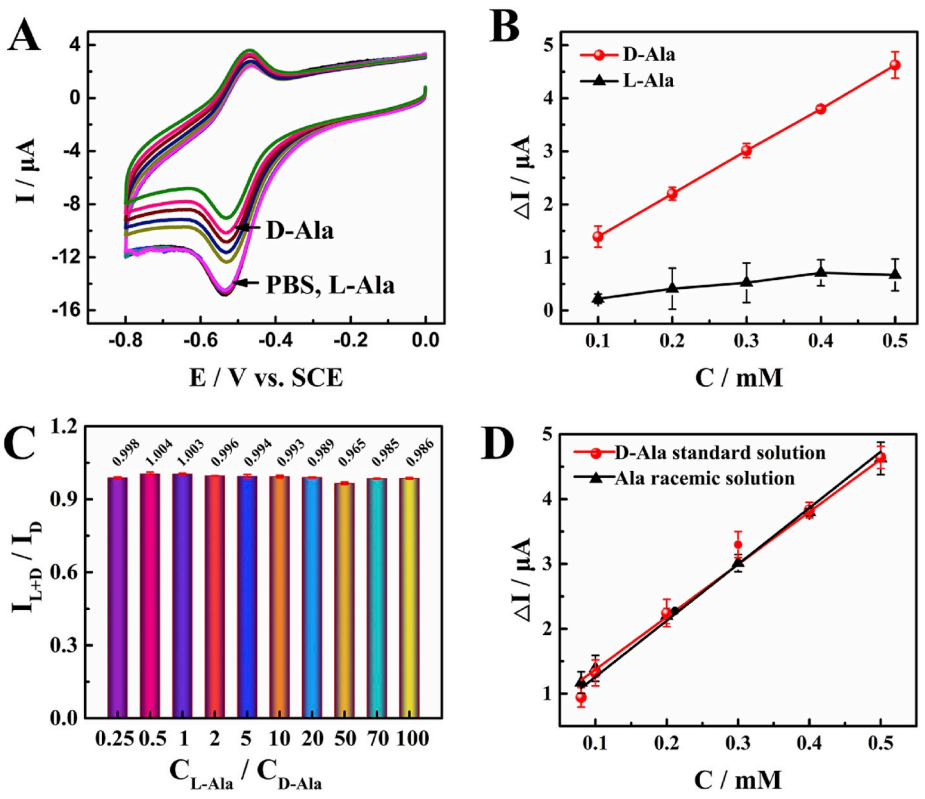

Fig. 6. (A) CV curves of DAAO/CNT/GCE in air-saturated PBS, air-saturated L-Ala and air-saturated D-Ala with concentrations of 0.1 mM, 0.2 mM, 0.3 mM, 0.4 mM and 0.5 mM. (B) Electric signal responses for DAAO/CNT/GCE in air-saturated L-Ala and D-Ala with concentrations of 0.1 mM, 0.2 mM, 0.3 mM, 0.4 mM and 0.5 mM. (C) Histogram of the electric signal ratio (I_{L+D}/I_D) of mixed Ala enantiomers (0.05 mM, 0.1 mM, 0.5 mM, 0.4 mM, 4 mM, 10 mM, 14 mM, and 20 mM LAA mixed with 0.2 mM D-Ala) to 0.2 mM D-Ala. (D) Linear relationship between the electric signal responses and the concentration of D-Ala in the standard D-Ala single solution and Ala-racemic solution.

biosensor based on DAAO can be used to estimate the total content of DAA in physiological fluids. The two main types of DAA in the human body are D-Ala and D-Ser, DAAO has a similar catalytic efficiency to that of these two DAAs, so using D-Ala as a standard, the total DAA content can be roughly estimated (Nieh et al., 2013).

Based on the above, we tested the dynamic change of D-Ala in milk with the standard-addition method. The recovery of 0.4 mM D-Ala added to a milk solution that was diluted 40 times with 50 mM PBS (pH 7.4) was 80.85%, and the RSD was 1.3% (n = 3). To analyse the total content of DAA, we evaluated the total content of DAA in human urine samples by using the proposed sensor at 134 μM, consistent with a previous report (Nieh et al., 2013). These results of practical analysis were satisfactory and indicating extensive applications of the proposed biosensor.

4. Conclusion

In conclusion, we constructed a non-mediator-style electrochemical biosensor based on DAAO for DAA chiral recognition without complex electron transfer processes. Chiral recognition was based on the specific catalysis of DAAO to DAA. This specific catalysis resulted in a linear decrease in the reduction peak current with the increase of DAA. The mechanism for the decrease of the reduction peak current was discussed for the first time and verified by CV experiments. The mechanism is also suitable for non-mediator-style electrochemical biosensors based on other oxidases and can provide guidance for the signal change mechanism of mediator-style electrochemical biosensors. Moreover, the high anti-LAA interference ability shows that the combination of stereospecificity and a catalytic reaction greatly improves the chiral recognition efficiency, so quantitative determination of D-Ala in Ala enantiomer mixtures can be successfully achieved. Finally, the satisfactory results of the practical analyses in milk and urine samples show potential applications for the proposed biosensor both in food testing and disease assessment.

Declaration of competing interest

The authors declare that they have no known competing financial interests or personal relationships that could have appeared to influence the work reported in this paper.

CRediT authorship contribution statement

Tingting Tian: Conceptualization, Methodology, Formal analysis, Writing - original draft. **Mingxia Liu:** Visualization. **Lixia Chen:** Investigation. **Fengjiao Zhang:** Writing - review & editing. **Xin Yao:** Conceptualization. **Hong Zhao:** Writing - review & editing. **Xiangjun Li:** Conceptualization, Supervision, Project administration, Writing - review & editing, Funding acquisition.

Acknowledgment

This work was supported by the Beijing Natural Science Foundation (2182083) and University of Chinese Academy of Sciences (Y954011).

Appendix A. Supplementary data

Supplementary data to this article can be found online at https://doi.org/10.1016/j.bios.2019.111971.

References

Afkhami, A., Kafrashi, F., Ahmadi, M., Madrakian, T., 2015. RSC Adv. 5, 58609–58615.
Alim, S., Vejayan, J., Yusoff, M.M., Kafi, A.K.M., 2018. Biosens. Bioelectron. 121, 125–136.
Andreu, R., Ferapontova, E.E., Gorton, L., Calvente, J.J., 2007. J. Phys. Chem. B 111, 469–477.
Arai, G., Noma, T., Hayashi, M., 1998. J. Electroanal. Chem. 452, 43–48.
Atta, N.F., Galal, A., Ahmed, Y.M., 2019. J. Electrochem. Soc. 166, B623–B630.
Bains, J.S., Oliet, S.H., 2007. Trends Neurosci. 30, 417–424.
Bao, L., Chen, X., Yang, B., Tao, Y., Kong, Y., 2016. ACS Appl. Mater. Interfaces 8, 21710–21720.

Bergantini, A., Abplanalp, M.J., Pokhilko, P., Krylov, A.I., Shingledecker, C.N., Herbst, E., Kaiser, R.I., 2018. Astrophys. J. 860, 108.
Britto, P.J., Santhanam, K.S.V., Rubio, A., 1999. Adv. Mater. 11, 154–157.
Challier, L., Miranda-Castro, R., Barbe, B., Fave, C., Limoges, B., Peyrin, E., Ravelet, C., Fiore, E., Labbé, P., Coche-Guérente, L., Ennifar, E., Bec, G., Dumas, P., Mavré, F., Noë, V., 2016. Anal. Chem. 88, 11963–11971.
Csapó, J., Csapó-Kiss, Z., Stefler, J., 1995. J. Dairy Sci. 78, 2375–2381.
Degani, Y., Heller, A., 1988. J. Am. Chem. Soc. 110, 2615–2620.
Dominguez, R., Serra, B., Reviejo, A.J., Pingarron, J.M., 2001. Anal. Biochem. 298, 275–282.
Dong, L., Zhang, Y., Duan, X., Zhu, X., Sun, H., Xu, J., 2017. Anal. Chem. 89, 9695–9702.
Du, D.Y., Yan, L.K., Su, Z.M., Li, S.L., Lan, Y.Q., Wang, E.B., 2013. Coord. Chem. Rev. 257, 702–717.
Feng, W., Liu, C., Lu, S., Zhang, C., Zhu, X., Liang, Y., Nan, J., 2014. Microchim. Acta. 181, 501–509.
Gandolfi, I., Palla, G., Marchelli, R., 1994. J. Food Sci. 59, 152–154.
Gholivand, M.B., Mohammadi-Behzad, L., 2015. Mater. Sci. Eng. C. Mater. Biol. Appl. 57, 77–87.
Gou, H., He, J., Mo, Z., Wei, X., Hu, R., Wang, Y., Guo, R., 2016. J. Electrochem. Soc. 163, B272–B279.
Gupta, S., Murthy, C.N., Prabha, C.R., 2018. Int. J. Biol. Macromol. 108, 687–703.
Hao, C., Qu, A., Xu, L., Sun, M., Zhang, H., Xu, C., Kuang, H., 2019. J. Am. Chem. Soc. 141, 1091–1099.
Hashimoto, K., Fukushima, T., Shimizu, E., Okada, S., Komatsu, N., Okamura, N., Koike, K., Koizumi, H., Kumakiri, C., Imai, K., Iyo, M., 2004. Prog. Neuro-Psychopharmacol. Biol. Psychiatry 28, 385–388.
Iannlello, R.M., Lindsay, T.J., Yacynych, A.M., 1982. Anal. Chem. 54, 1098–1101.
Ishiwata, S., Hattori, K., Sasayama, D., Teraishi, T., Miyakawa, T., Yokota, Y., Matsumura, R., Nishikawa, T., Kunugi, H., 2018. J. Affect. Disord. 226, 155–162.
Kang, X., Wang, J., Wu, H., Aksay, I.A., Liu, J., Lin, Y., 2009. Biosens. Bioelectron. 25, 901–905.
Katz, E., Willner, I., 2004. ChemPhysChem 5, 1084–1104.
Kiss, D.J., Ferenczy, G.G., 2019. Org. Biomol. Chem. 17, 7973–7984.
Liu, Q., Chen, L., Zhang, Z., Du, B., Xiao, Y., Yang, K., Gong, L., Wu, L., Li, X., He, Y., 2017. Sci. Rep. 7, 1–9.
Liu, Q., Lu, X., Li, Jun, Yao, X., Li, Jinghong, 2007. Biosens. Bioelectron. 22, 3203–3209.
Liu, S., Ju, H., 2003. Biosens. Bioelectron. 19, 177–183.
Liu, Y., Wang, M., Zhao, F., Xu, Z., Dong, S., 2005. Biosens. Bioelectron. 21, 984–988.
Moreno-Guzmán, M., García-Carmona, L., Molinero-Fernández, Á., Cava, F., López Gil, M.Á., Escarpa, A., 2017. Sens. Actuators B Chem. 242, 95–101.
Moreno, J.A., Montes, F.J., Catalán, J., 1996. Enzym. Microb. Technol. 18, 379–382.
Mothet, J.P., Parent, A.T., Wolosker, H., 2000. Proc. Natl. Acad. Sci. 97, 4926–4931.
Nieh, C.H., Kitazumi, Y., Shirai, O., Kano, K., 2013. Biosens. Bioelectron. 47, 350–355.
Nugent, J.M., Santhanam, K.S.V., Rubio, A., Ajayan, P.M., 2001. Nano Lett. 1, 87–91.
Pernot, P., Mothet, J.P., Schuvailo, O., 2008. Anal. Chem. 80, 1589–1597.
Pollegioni, L., Molla, G., Sacchi, S., Rosini, E., Verga, R., Pilone, M.S., 2008. Appl. Microbiol. Biotechnol. 78, 1–16.
Pundir, C.S., Lata, S., Narwal, V., 2018. Biosens. Bioelectron. 117, 373–384.
Quan, Z., Song, Y., Feng, Y., LeBlanc, M.H., Liu, Y.M., 2005. Anal. Chim. Acta 528, 101–106.
Sa, Y.J., Kim, J.H., Joo, S.H., 2019. Angew. Chem. Int. Ed. 58, 1100–1105.
Sacchi, S., Pollegioni, L., Pilone, M.S., 1998. Biotechnol. Tech. 12, 149–153.
Tao, Y., Gu, X., Yang, B., Deng, L., Bao, L., Kong, Y., Chu, F., Qin, Y., 2017. Anal. Chem. 89, 1900–1906.
Tohala, L., Oukacine, F., Ravelet, C., Peyrin, E., 2015. Anal. Chem. 87, 5491–5495.
Wcislo, M., Compagnone, D., Trojanowicz, M., 2007. Bioelectrochemistry 71, 91–98.
Wu, D., Kong, Y., 2019. Anal. Chem. 91, 5961–5967.
Wu, T., Wei, X., Ma, X., Li, J., 2017. Microchim. Acta 184, 2901–2907.
Zaidi, S.A., 2017. Biosens. Bioelectron. 94, 714–718.
Zain, Z.M., O'Neill, R.D., Lowry, J.P., Pierce, K.W., Tricklebank, M., Dewa, A., Ab Ghani, S., 2010. Biosens. Bioelectron. 25, 1454–1459.
Zhang, L., Song, P., Long, H., Meng, M., Yin, Y., Xi, R., 2017. Sens. Actuators B Chem. 248, 682–689.
Zhang, M., Smith, A., Gorski, W., 2004. Anal. Chem. 76, 5045–5050.
Zhang, Q., Fu, M., Lu, H., Fan, X., Wang, Haiyang, Zhang, Y., Wang, H., 2019. Sens. Actuators B Chem. 296, 126667.
Zhu, S., Lin, X., Ran, P., Mo, F., Xia, Q., Fu, Y., 2017. Microchim. Acta 184, 4679–4684.